

Comparison of cooling effect between green space and water body

Xingyu Tan ^a, Xiang Sun ^{a,*}, Chengdao Huang ^a, Yuan Yuan ^a, Donglin Hou ^b

^a School of Resources, Environment and Materials, Guangxi University, 530004, Nanning, China

^b Policy Research Centre for Environment and Economy, Ministry of Ecology and Environment of the People's Republic of China, Beijing, 100029, China



ARTICLE INFO

Keywords:

Urban heat island
Green space
Water body
Cooling range
Cooling intensity

ABSTRACT

The cooling effects of green spaces and water bodies are essential in subtropical cities with high temperatures combined with increasing urban heat island effect, while there is insufficient research on the difference between these two categories of cold sources. Therefore, Nanning, China, was selected as the typical case in the subtropical climate zone, and spatial and statistical analysis based on Landsat 8 OLI/TIRS images was conducted to compare the cooling effect and factors of blue and green spaces. Results showed that (1) the area-related green-space and water-body metrics are significantly positively correlated with the cooling effect. An additional 10 % of green space cover leads to a decline in the mean LST of 0.39 °C compared with a decline of 0.42 °C for water cover; (2) green and blue spaces with simple shapes and high fragmentation may have strong cooling effect, whereas green and blue spaces with more complex shapes may cool larger areas, benefiting more residents; (3) the threshold values of efficiency (TVoE) of tree-based green spaces and water patches were both approximately 0.30 ha, increasing with spatial sprawl of impervious surfaces; and (4) water bodies have slightly higher cooling intensity and much larger cooling ranges than tree-based green spaces.

1. Introduction

The urban heat island (UHI) effect due to rapid urbanization is a significant climatic phenomenon, and poses a series of challenges to humans, including impairing of urban residents' physical and mental health, accelerating energy consumption, and promoting unsustainable urban development (Akbari & Kolokotsa, 2016; Cao, Yu, Georgescu, Wu, & Wang, 2018; Sun & Augenbroe, 2014). Consequently, a multitude of measures have been proposed to improve the thermal environment. It is widely acknowledged that urban blue-green spaces are effective and environmentally friendly for alleviating the aggravating UHI effect and reducing the detrimental consequences of increasing temperatures (Amani-Beni, Zhang, Xie, & Xu, 2018; Brown, Vanos, Kenny, & Lenzholzer, 2015; Moss, Doick, Smith, & Shahrestani, 2019; Sun, Chen, & Braat, 2017; Zhang, Murray, & Turner, 2017; Zhou, Qian, Li, Li, & Han, 2014). Urban blue-green systems mainly consist of green spaces and water bodies (Wu, Wang, Fan, & Xia, 2018). Due to the greater heat capacity of water than air and other materials on the land surface (Cai, Han, & Chen, 2018), blue spaces always have lower temperatures than other spaces during the daytime. In addition, green spaces create cooling islands through direct shading and evapotranspiration by vegetation in

cities (Gunawardena, Wells, & Kershaw, 2017; Kong, Yin, James, Hutyra, & He, 2014). Moreover, through the exchange of air convection and diffusion, the cooler air within blue-green spaces blows to the surrounding areas and achieves a cooling effect around these spaces (Doick, Peace, & Hutchings, 2014; Hamada & Ohta, 2010; Murakawa, Sekine, Narita, & Nishina, 1991; Yan, Wu, & Dong, 2018). The cooling effect extending into adjacent areas is generally reflected by the cooling range and cooling intensity of green and blue spaces, referring to the horizontal distance where the cooling effect is present and the maximum temperature difference in the spaces and surroundings (Topalar, Blocken, Maiheu, & Heijst van, 2018).

As two categories of cooling islands, the cooling range and cooling intensity of green spaces or water bodies in different regions and seasons have been investigated and identified extensively (Amani-Beni et al., 2018; Du et al., 2016, 2017; Huang, Cui, & He, 2018; Xue et al., 2019; Yu, Guo, Jørgensen, & Vejre, 2017). In addition, there is increasing interest in exploring the factors influencing their cooling effect for the benefits of maximizing the cooling effect under the circumstance of a severe UHI effect (Chen, Yao, Sun, & Chen, 2014; Kong et al., 2014; Zhang et al., 2017; Zhou, Cao, & Wang, 2019). The cooling effect of green spaces and water bodies is impacted not only by external factors,

* Corresponding author at: School of Resources, Environment and Materials, Guangxi University, Daxue East Road 100, Nanning City, Guangxi Province, China.

E-mail addresses: 1060229179@qq.com (X. Tan), sunxiangphd@gxu.edu.cn (X. Sun), 939801488@qq.com (C. Huang), 2742608235@qq.com (Y. Yuan), 1002402054@qq.com (D. Hou).

such as spatial locations, land cover features, and surrounding building density (Cai et al., 2018; Hathway & Sharples, 2012) but also, by different landscape characteristics (Chang, Li, & Chang, 2007; Lau, Lin, & Qin, 2012; Lee, Lee, Jin, & Song, 2009; Monteiro, Doick, Handley, & Peace, 2016). It is more feasible and convenient for urban planners to regulate green-space or water-body characteristics than external conditions to enhance the cooling effect extending to the surroundings and benefit more urban residents. For green spaces, it is generally accepted that a larger size confers a higher cooling effect (Ca, Asaeda, & Abu, 1998; Feng & Shi, 2012; Jaganmohan, Knapp, Buchmann, & Schwarz, 2016; Jauregui, 1991; Yu et al., 2017). In addition, green space patches with simple shapes were found to have a more obvious cooling effect than those with complex shapes (Huang et al., 2018; Kong et al., 2014), while other studies proposed the opposite (Asgarian, Amiri, & Sakieh, 2015; Estoque, Murayama, & Myint, 2017). Meanwhile, the fragmentation or aggregation of green spaces was demonstrated to impact their cooling effect (Bao, Li, Zhang, Zhang, & Tian, 2016; Xie, Wang, Chang, Fu, & Ye, 2013). Moreover, tree-based green spaces were discovered to have the greatest cooling effect, followed by bushes and grasslands (Kong et al., 2014). For water bodies, the characteristics of their area, shape complexity, fragmentation and others were also identified to be correlated with their cooling effect (Du et al., 2016; Sun & Chen, 2012; Syafii et al., 2017; Xue et al., 2019). By comparing the cooling effects of green spaces and water bodies, there were a few inconsistencies in the conclusions. Lin, Yu, Chang, Wu, and Zhang (2015) concluded that the cooling effect of water bodies was slightly stronger than that of green spaces in Beijing, China. The review by Yu, Guo, and Sun (2015) revealed that the cooling effect of green space was stronger than that of water bodies in May, but the opposite was found in November. Another case study by Yang, Yu, Jørgensen, and Vejre (2020) showed a greater cooling effect of water bodies than that of green space in all four seasons in high latitude regions. However, systematic comparisons of the cooling effects of green spaces and water bodies and their influencing factors at the patch and landscape levels within a given city with a subtropical climate have not been fully addressed. Moreover, urban planners are eager to determine what percentage of blue-green infrastructure should be planned within a given administrative regulation area to meet the needs for a cooling effect for urban residents. Is it better to plan patches of blue-green infrastructure with bigger size? What is the optimal patch size of blue-green infrastructure? Should the patches of blue-green infrastructure be planned to be distributed more compactly or

fragmentally? The linkage between the theoretical studies of cooling effects and implementation practices has not been fully discussed.

Therefore, with a subtropical city, Nanning, as our selected typical case, the main objectives of this study were to (1) explore the differences in the cooling effect between urban green and blue spaces; (2) compare the differences in the landscape factors with a dominant influence on the cooling effect and the quantitative impacts of the same dominant landscape factors on the cooling effect of urban green and blue spaces; and (3) provide possible implications for urban green and blue space planning in Nanning and other cities in the same subtropical climate zone.

2. Methodology

2.1. Study area

Nanning ($107^{\circ}45' E \sim 108^{\circ}51' E$, $22^{\circ}13' N \sim 23^{\circ}32' N$), the capital of Guangxi Province, China, is in southern China (Fig. 1a). Nanning has an area of $22,112 \text{ km}^2$ and a permanent population of approximately 7.15 million (Nanning Municipal Statistics Bureau, 2018). This city belongs to a humid subtropical monsoon climate zone with a long summer and short winter in a year. Nanning had the mean and highest air temperatures of 32.97°C and 37.00°C in June, July, and August from 2016–2019, indicating a severe thermal environment in this city. The dominant vegetation types are tropical and subtropical evergreen broadleaf trees. In addition, Nanning is characterized by abundant plant resources and is known as the green city of China. To date, the area of forests has reached 10543.40 km^2 , the forest coverage is 48.73 %, and the per capita park green space in Nanning has increased rapidly, reaching 13.34 m^2 by 2019 (Nanning Municipal Administration Bureau, 2019). This study concentrated on the urbanized area of central Nanning city with an area of approximately 240 km^2 (Fig. 1b).

2.2. Data collection and processing

2.2.1. Data sources

Due to data limitations (the images from June to September over the past two decades were found to be covered by too many clouds) in Nanning, three Landsat 8 OLI/TIRS satellite images with highly clear atmospheric conditions acquired on October 9, 2016, October 31, 2018, and October 2, 2019 were selected in this study. These images were all

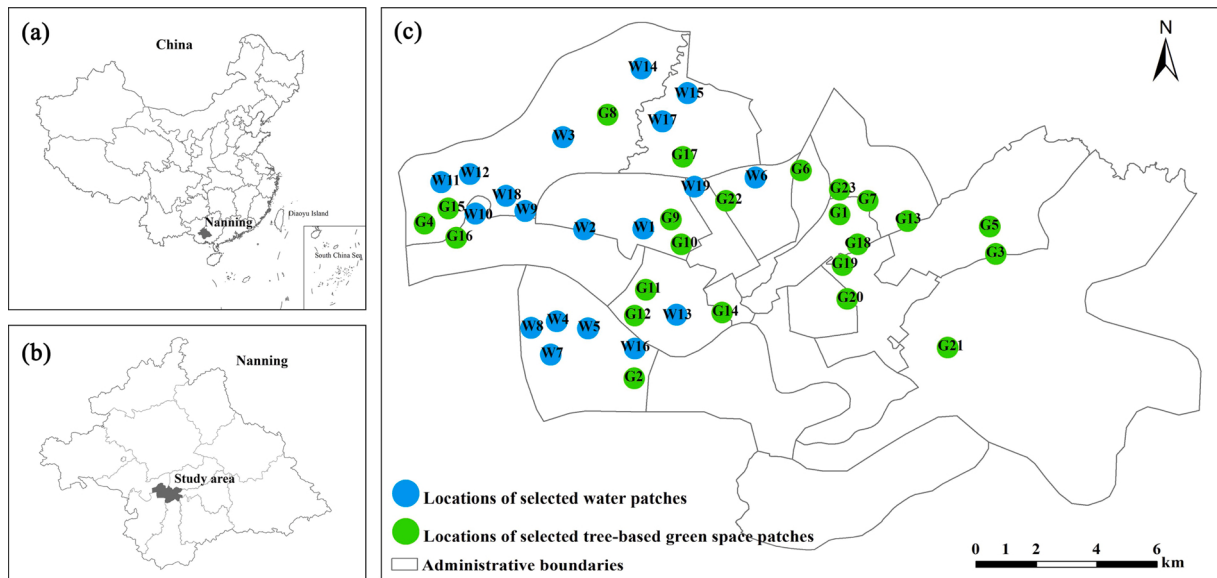


Fig. 1. (a-c) Location of (a) Nanning city in China, (b) our study area in Nanning city, and (c) selected tree-based green space and water patches in the study area. (For interpretation of the references to colour in this figure legend, the reader is referred to the web version of this article).

obtained from the remote sensing data sharing website (<http://glovis.usgs.gov/>) maintained by the United States Geological Survey (USGS). Meanwhile, according to the historical meteorological data from <http://qx.nanning.gov.cn/>, the lowest and highest average temperatures were 21.33 °C and 33.33 °C for the aforementioned three days in October, which showed no significant differences from the historical temperatures in Nanning in summer (June, July, and August) from 2016 to 2019 (25.41 °C and 33.23 °C for the lowest and highest). Furthermore, considering the long summer from April to October in Nanning, it is feasible to use these three satellite images to investigate the cooling effects of green spaces and water bodies.

2.2.2. Land surface temperature (LST) retrieval and land cover identification

First, the digital number (DN) values of the thermal infrared band (Bands 10 and 11 in Landsat TIRS) were transformed into spectral radiance values. Second, we derived the brightness temperatures from spectral radiance values. Finally, the real LST data were obtained by converting the brightness temperatures. Here, the real LST of the study area was calculated using Eq. (1) (Artis & Carnahan, 1982).

$$T_s = \frac{T}{1 + (\lambda T / \rho) \ln e} \quad (1)$$

where T_s is the real LST and T is the brightness temperature, derived from Eq. (2) (NASA, 2021); λ is the wavelength of emitted radiance ($\lambda = 10.9 \mu\text{m}$, the center wavelength of Landsat 8 Band 10, was used); $\rho = 1.438 \times 10^{-2} \text{ mK}$; and e is the land surface emissivity, estimated according to Qin, Li, Gao, and Zhang (2006).

$$T = \frac{K_2}{\ln(\frac{K_1}{L_\lambda} + 1)} \quad (2)$$

where K_1 and K_2 are Planck constants. $K_1 = 774.89 \text{ W m}^{-2} \text{ sr}^{-1} \mu\text{m}^{-1}$ and $K_2 = 1321.08 \text{ K}$ for Landsat 8 Band 10 data (Chander et al., 2004). L_λ is the spectral radiance, obtained using Eq. (3).

$$L_\lambda = Gains \times DN + Offsets \quad (3)$$

where *Gains* is the gain coefficient; *DN* is the digital number of the thermal infrared band; and *Offsets* is the offset coefficient. *Gains* and *Offsets* were obtained from the header file. Fig. 2 shows the results of the

retrieved LSTs.

Four typical categories of land cover (green space, water, bare land, and impervious surface) were mapped in Fig. 2 using the knowledge classification module in ERDAS software (9.2). Then, an accuracy assessment was carried out to verify the classification quality based on kappa coefficients and overall accuracies. The kappa statistics of 0.8750 to 0.9167 and overall accuracies of 90.63%–93.75% manifest the ideal results. The impervious surface has the highest proportion in all years, increasing from 57.16%–62.29% from 2016 to 2019. However, the percentages of green space and water cover decrease from 20.37 % to 13.45 % and from 9.36 % to 8.04 %, respectively. Green space and water patches with their surroundings were identified by artificial visual interpretation based on high-resolution Google Earth images.

2.3. Sample selection and landscape characterization

At the patch level, to avoid interactions of the cooling effect produced by green space and water patches and improve analytical reliability, some principles and rules were set for the selection of green space and water patch samples as follows and shown in Fig. 3: (1) to select tree-based green space patches with vegetation coverage of more than 80%; (2) to select green space patches without water patches inside and more than 300 m away from any other green space or water patches to avoid interactions among samples; (3) to select water patches more than 300 m away from any other green space or water patches to avoid interactions among samples; and (4) to select samples with different variations in area and shape. Based on these principles, 23 tree-based green space patches and 19 water patches were selected in this study (Fig. 1c, the locations and characteristics of these patches did not change from 2016 to 2019 based on high-resolution Google Earth images), and patches with areas of less than 900 m² were excluded.

At the landscape level, considering the resolution of Landsat 8 images and the total area of 240 km² of our study area, three grid sizes (300 m × 300 m, 600 m × 600 m and 900 m × 900 m) were tested to determine the optimal grid size to examine the impacts of green-space and water-body landscape metrics on the mean LST within the analysis grid cells. Excluding large parks, lakes, and rivers, the area of green spaces and water bodies in the study area is approximately 2–3 ha and up to more than 10 ha. If the grid size is small (i.e., 300 m × 300 m, the same as 9 ha), those large patches will be divided into small parts by the grid, and then the cooling effect caused by them will be estimated with

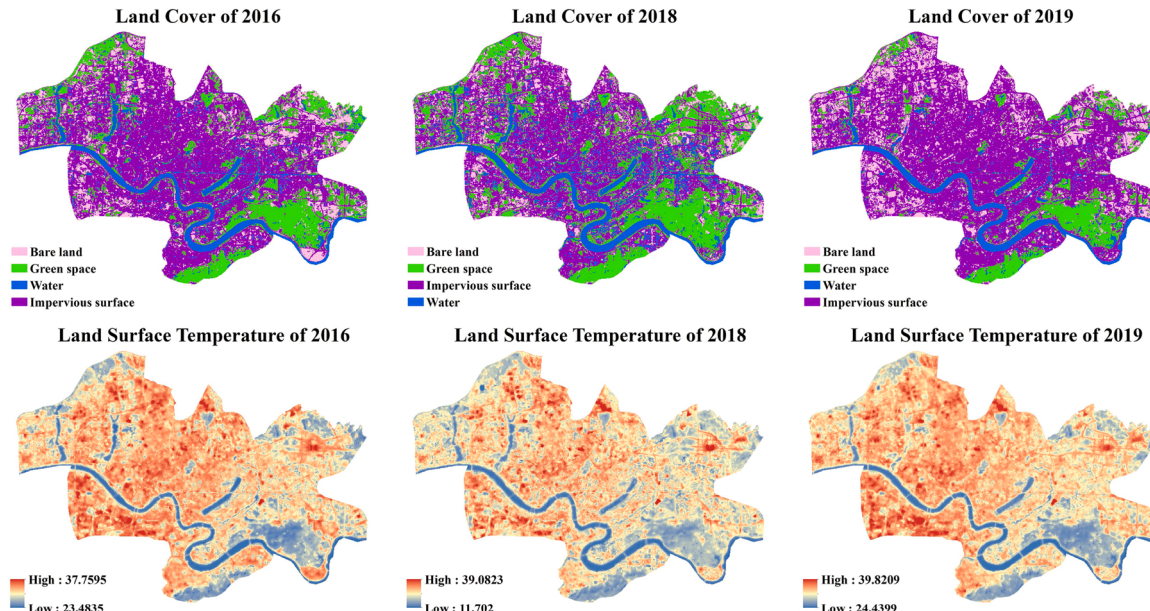


Fig. 2. Spatial distribution of land surface temperature and land cover of the study area.

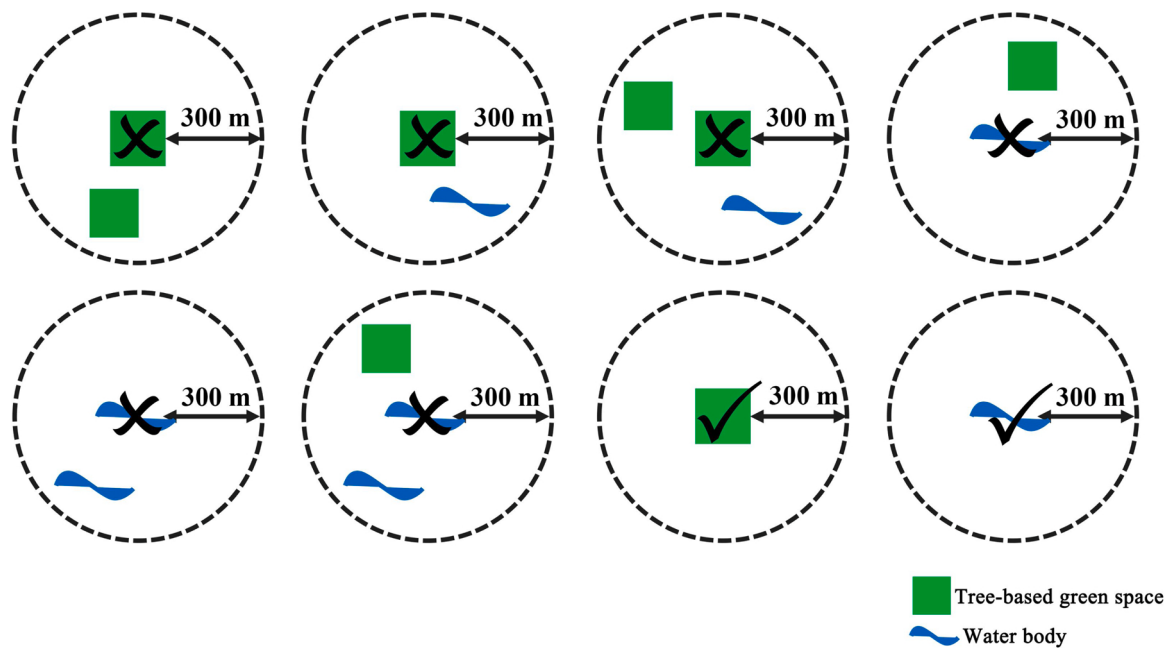


Fig. 3. Schematic diagram of sampling principles. Tree-based green space and water patches marked with 'x' are those not suitable for sample selection, and those marked with '✓' are suitable for sample selection. (For interpretation of the references to colour in this figure legend, the reader is referred to the web version of this article).

potential bias. However, if a grid size that is too large is chosen, the cooling effect of small green spaces or water bodies within grids will be nonsignificant or even ignored. Furthermore, a large grid size will result in insufficient samples. Meanwhile, significant relationships existed between the percentage of green space and water body (PLAND) and mean LST ([Fig. 4](#)), with relatively good fits ($R^2 = 0.36, 0.33$) when a grid size of $600 \text{ m} \times 600 \text{ m}$ was applied. Therefore, $600 \text{ m} \times 600 \text{ m}$ was chosen to conduct the subsequent analysis. In particular, grids that contained only 'bare land' and/or 'impervious surface' were not included.

Six metrics at the patch and landscape level from the aspects of area, shape complexity, fragmentation and aggregation were chosen to characterize the green space and water landscape patches and to analyze the relationship between these characteristics and the cooling effect ([Table 1](#)): area, patch shape index (PSI), percentage of landscape (PLAND), mean patch shape index (SHAPE_MN), mean patch fractal dimension (FRAC_MN), and aggregation index (AI). All landscape metrics were calculated by FRAGSTATS (4.2).

2.4. Quantifying the cooling effect of tree-based green space and water patches

To calculate the cooling effect of tree-based green space and water patches, buffer zones were built from the edges of selected patches at intervals with fixed widths (30 m). The mean LST of each buffer zone was regarded as the LST at the corresponding distance. The cooling range is the distance from the edge of the patch and the first turning point on the temperature curve ([Fig. 5a](#)). The cooling intensity is the temperature drop of the first turning point compared to the mean temperature of the patch edge ([Du et al., 2016](#); [Lin et al., 2015](#); [Sun, Chen, Chen, & Lü, 2012](#)). Cooling intensity is positively correlated with patch size, while as the area further increases, the increase in cooling intensity slows down and then stabilizes within a certain range ([Yu et al., 2017](#)). As logarithmic regression is used to approximately characterize the relationship between cooling intensity and patch area, the threshold value of efficiency (TVoE) occurs at the point where the slope of the resulting logarithmic function equals 1 ([Fig. 5b](#)), based on which the corresponding area is the optimal patch size for urban planners ([Fan](#)

[et al., 2019](#)).

2.5. Statistical analysis

First, Pearson correlations were carried out to examine the relationships between the mean LST and landscape characteristics of green spaces and water bodies. Due to the probable high correlations between some landscape metrics, spurious relationships may be obtained between the mean LST and metrics. Therefore, partial correlation analysis should be conducted to investigate their relationships after controlling the influence of certain landscape metrics. Then, the ordinary least-squares (OLS) method was used to estimate the contribution of landscape metrics to the LST changes.

In addition, nonlinear regression analyses were also performed to fit the relationships between the characteristics of tree-based green space and water patches and their cooling effect. SPSS 23.0 and Origin 8.0 software were utilized for all statistical analyses.

3. Results

3.1. Characteristics and cooling effect of selected tree-based green space and water patches

[Fig. 6](#) displays the LST curves of the first 4 tree-based green spaces and 4 water patches in 2019 as examples, indicating that the LST around the green space and water patches increases as the distance to them increases. However, with further increase in the distance, the LST reaches its maximum value, which implies that the cooling range is reached and the cooling intensity is obtained.

For the 23 tree-based green space patches, the area is between 0.12 and 10.27 ha with an average value of 2.63 ha, and the PSI is between 1.41 and 3.05 with an average of 2.84. For the 19 water patches, the area is between 0.14 and 10.79 ha with an average value of 1.86 ha, and the PSI is between 1.19 and 2.74 with an average of 2.07.

In addition, in terms of their cooling effect, the cooling range of tree-based green space patches ranges from 60 to 270 m with an average value of 140 m, while the cooling range of water patches is between 60 and 390 m with an average of 180 m. Furthermore, the cooling intensity

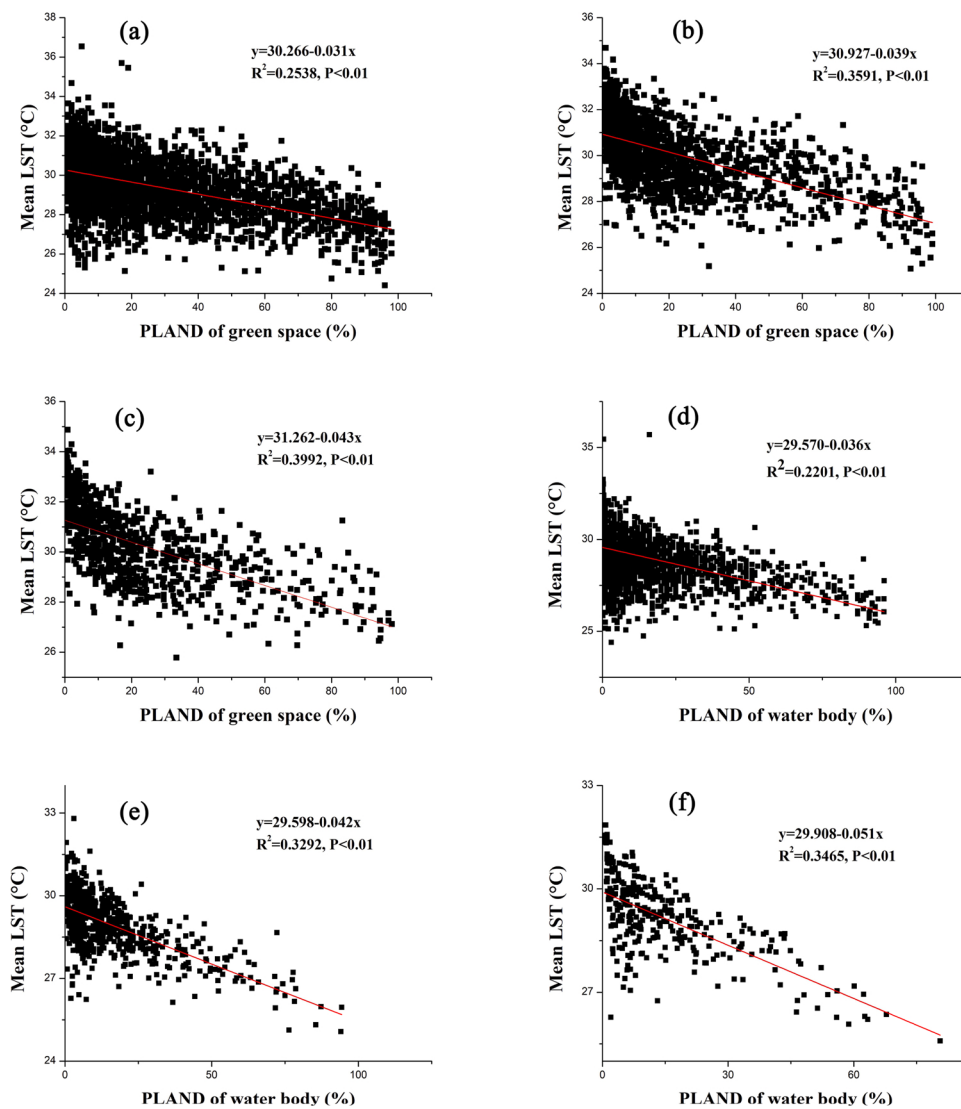


Fig. 4. (a-c) Relationship between the percentage of landscape (PLAND) of green space and mean LST (°C) in different grid sizes: (a) 300 m × 300 m, (b) 600 m × 600 m, and (c) 900 m × 900 m. (d-f) Relationship between the percentage of landscape (PLAND) of water body and mean LST (°C) in different grid sizes: (d) 300 m × 300 m, (e) 600 m × 600 m, and (f) 900 m × 900 m. (For interpretation of the references to colour in this figure legend, the reader is referred to the web version of this article).

Table 1
Landscape metrics at the patch level and landscape level used in this study.

Metric	Definition	Range
Patch Level		
Area (a)		a ≥ 0
Patch shape index (PSI)	$PSI = \frac{e}{2 \times \sqrt{\pi a}}$	PSI ≥ 1
Landscape Level		
Percentage of landscape (PLAND)	$PLAND = \frac{\sum_{i=1}^n a_i}{A} \times 100\%$	0 < PLAND < 100
Mean patch shape index (SHAPE_MN)	The average PSI of all patches of the corresponding patch type	SHAPE_MN ≥ 1
Mean fractal dimension (FRAC_MN)	$FRAC = \frac{2 \times \ln[f/(0.25e)]}{\ln a}$	1 ≤ FRAC_MN ≤ 2
Aggregation index (AI)	The number of like adjacencies involving the corresponding class, divided by the maximum possible number of like adjacencies involving the corresponding class, which is achieved when the class is maximally clumped into a single, compact patch; multiplied by 100 (to convert to a percentage)	0 ≤ AI ≤ 100

e is the length of the edge (or perimeter) of patch; a is the area of the patch; n is the total number of patches; and A is the total area of the landscape.

of tree-based green space patches is between 0.11 and 1.75 °C with an average value of 0.87 °C, but the cooling intensity of water patches ranges from 0.08 and 2.02 °C with an average of 0.88 °C.

3.2. Landscape-metric impacts on the cooling effect of tree-based green space and water patches

At the patch level, different correlations were identified between the two landscape metrics (area and PSI) and the cooling effect, including the cooling range and cooling intensity (Table 2). For both tree-based green spaces and water patches, positive correlations are apparent between the area and cooling effect (cooling range and cooling intensity). However, the cooling ranges and intensity of tree-based green space and water patches seem not to be relevant to their shape complexity (quantified as PSI). As a result, in terms of the two main characteristics of green space and water patches, the area has the greatest impact on their cooling effect, while the shape complexity virtually makes no difference.

As a significantly associated factor, the tree-based green space patch area has a logarithmic relationship with their cooling effect (Fig. 7), indicating that the cooling effect starts to increase rapidly as the patch area increases within a certain range but finally tends to level off. The same relationship was discovered between the water patch area and their cooling ranges and intensity. From 2016–2019, the tree-based

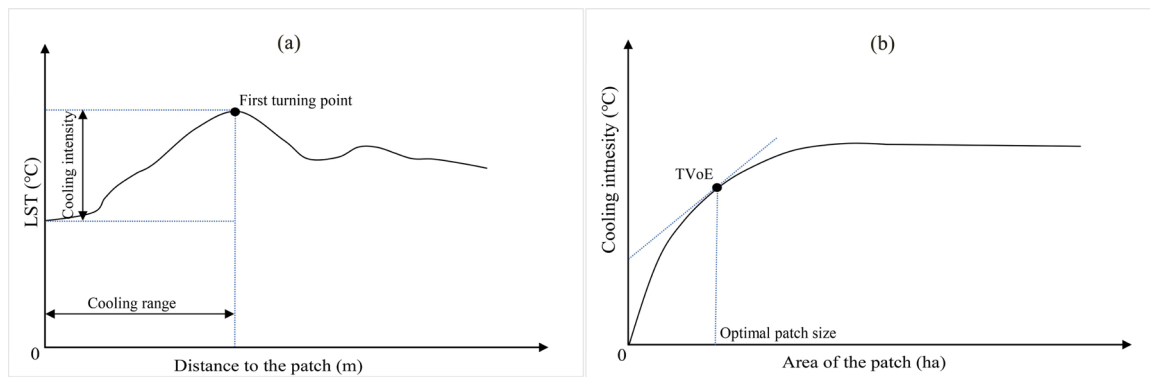


Fig. 5. (a-b) Curve modeling and tipping point detection. (a) LST and distance to the patch to interpret the cooling range and cooling intensity and (b) cooling intensity and area of the patch to show the cooling efficiency, TVoE, and optimal patch size.

green space and water patches seemed to show significant cooling intensity. The cooling ranges of tree-based green space and water patches also manifest the same extending trend, excluding the farther cooling range of tree-based green space patches within 0–1.27 ha in 2018 than that in 2019. Meanwhile, there was an increasing trend in the TVoE of both tree-based green space and water patch area from 2016 to 2019. According to Fig. 8, the mean TVoE of tree-based green space and water patch area were found to be approximately 0.32 ha and 0.31 ha, respectively. Compared to tree-based green space patches, water patches with the same area exhibit a slightly higher cooling intensity and much farther cooling range.

3.3. Influence of green-space and water-body landscape metrics on the LST of urbanized areas

For both green spaces and water bodies, highly positive correlations between the area-related metric (PLAND) and temperature reduction are apparent (Table 3). Additionally, significant positive impacts of landscape shape complexity (quantified as SHAPE_MN and FRAC_MN) on the mitigation of the thermal environment in urbanized areas were discovered. In addition, more aggregated green spaces and water bodies seem to lead to a lower mean LST of the surroundings. Due to the high correlations between the four metrics, further partial correlations in Table 3 display the respective effects of PLAND, SHAPE_MN, FRAC_MN, and AI on the mean LST after controlling other landscape metrics. A significant positive influence of PLAND on the temperature reduction still exists, while negative correlations between SHAPE_MN, AI and the LST drop were identified, manifesting that simpler shapes and more fragmented green spaces or water bodies may be preferable for reducing surrounding LSTs.

As reported by the OLS results (Fig. 4), an additional 10 % PLAND of green spaces is statistically associated with a decline in the mean LST of 0.39 °C, which is significant at the 1% level, while the same increase in the PLAND of water bodies leads to a slightly higher decrease (0.42 °C) in the mean LST of the surroundings.

4. Discussion

4.1. Difference in cooling range and cooling intensity between green spaces and water bodies

In the subtropical climate zone, the high temperature combined with the UHI effect makes the cooling effect of green spaces and water bodies more essential. As different kinds of cold sources, green spaces and water bodies provide cooling effects in different ways (Cai et al., 2018; Gunawardena et al., 2017; Kong et al., 2014), which may be the fundamental reason for the difference in cooling effects between green spaces and water bodies. A few studies have also reported this

difference. Lin et al. (2015) and Yu, Guo, Zeng, Koga, and Vejre (2018) noted that water bodies have higher cooling efficiency than green spaces. According to Yu et al. (2015), the cooling effect of water bodies is stronger than that of green space in November, and green space cooling is stronger than that of the water bodies in May. In this study, we obtained a slightly higher cooling intensity and much farther cooling range of the water body than that of the tree-based green space in October from 2016–2019, which is in line with the conclusion that the cooling intensity and extent of water bodies are greater than those of green spaces in the four seasons by Yang, Yu, Jørgensen, and Vejre (2020). Furthermore, the TVoE of tree-based green space and water patches increases year by year with the increasing proportion of impervious surfaces in urbanized areas, implying that a green space or water patch with a large area is needed to obtain the most efficient cooling intensity.

4.2. Comparison of landscape-metric influence on the cooling effect of green spaces and water bodies

Previous studies have revealed that the characteristics of the cooling effects of green spaces and water-bodies are mainly composed of area, shape complexity, and aggregation (Masoudi, Tan, & Liew, 2019; Masoudi & Tan, 2019). At the landscape level, for both green spaces and water bodies, this study showed that their proportion (PLAND) is a significant determinant of LST in urbanized areas. Our results also emphasize the important roles of shape complexity and aggregation of green spaces and water bodies in determining LST. Furthermore, the positive correlation between the proportions of green-spaces and water-bodies and temperature reduction is apparent, which verifies the results found in many previous studies (Chen, Zhao, Li, & Yin, 2006; Li, Zhou, Ouyang, Xu, & Zheng, 2012; Oliveira, Andrade, & Vaz, 2011; Zhang, Odeh, & Ramadan, 2013; Zhou & Wang, 2011). Meanwhile, with the same area, green spaces and water bodies with more fragmentation and simpler shapes also result in lower LST of the surroundings, which is supported by several studies (Bao et al., 2016; Li et al., 2011; Maimaitiyiming et al., 2014). At the patch level, whether for tree-based green space patches or water patches, highly positive correlations prevail between area and their cooling ranges and intensity. Moreover, the PSI of tree-based green spaces and water patches is found not to be associated with their cooling ranges and intensity. Generally, it is accepted that a larger area, water capacity or NDVI results in the strengthening of the cooling capacity of green space and water patches (Buyantuyev & Wu, 2010; Fan et al., 2019; Wu et al., 2018; Zhang et al., 2013). Although the change in the PSI (its shape becomes simpler or more complex) of a specific green space or water patch has no effect on its cooling capacity, green spaces and water bodies with more complex shapes will create more extensive cooling areas within a landscape. For example, as shown in Fig. 9, based on the cooling range of 200 m, 11.24 ha of blue-green

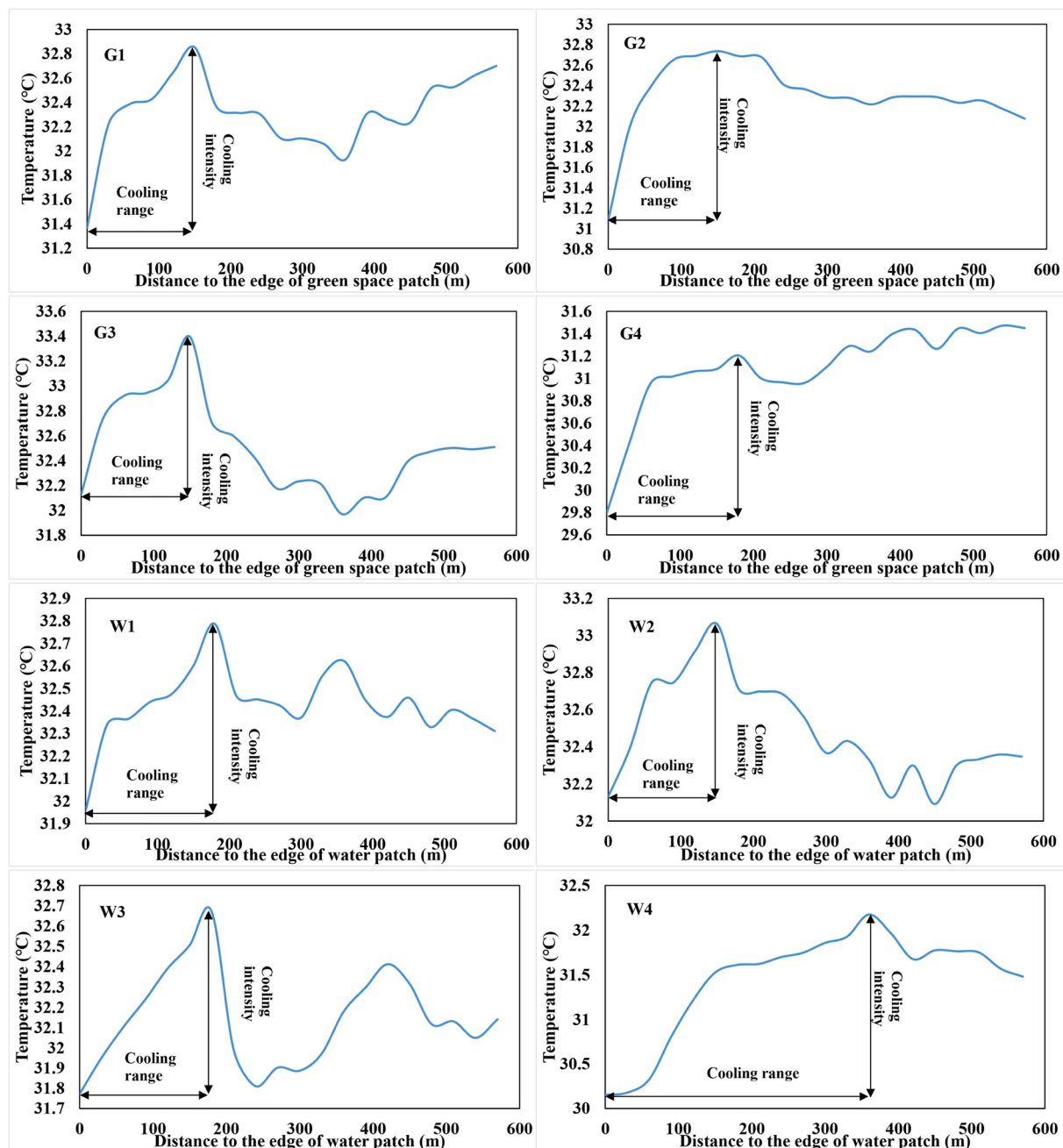


Fig. 6. Land surface temperature (LST) curves based on buffer zone analysis for the 4 selected tree-based green spaces and 4 water patches. (For interpretation of the references to colour in this figure legend, the reader is referred to the web version of this article).

Table 2

Pearson correlation coefficients between the cooling effect and landscape metrics at the patch level.

Cooling effect	Green space patch area	PSI of green space patch	Water patch area	PSI of water patch
Cooling intensity	0.825**	0.142	0.709**	0.509
Cooling range	0.804**	0.059	0.792**	0.265

**Correlation is significant at the 0.01 level (2-tailed).

landscape patch A with a PSI of 2.56 ('S'-shape) can provide a cooling effect to 63 ha of surrounding areas, while the cooling area of landscape patch B with the same area as A but a PSI of 1.13 (regular rectangle) is

only 40 ha, demonstrating that the more complex the landscape patch is, the larger the cooling area and the more residents benefited.

Except for the characteristics of green spaces and water bodies themselves, external factors, such as times, spatial locations, and surrounding land cover features, are also likely to be responsible for changes in the green-space and water-body cooling effects. For example, the cooling effect of a green area in Japan at night could extend 200–300 m from its border, while the cooling range in the day was reported as 300–500 m by Hamada and Ohta (2010); the cooling extent of 197 water bodies in Beijing was found to vary not only with the area and geometry but also with their locations and surrounding built-up proportions (Sun & Chen, 2012); the cooling effect of a large urban park with the area of 680 ha reached 1.4 km from the western edge due to low building density, whereas the cooling range from the park's eastern edge was discovered to be small where the building density was relatively high

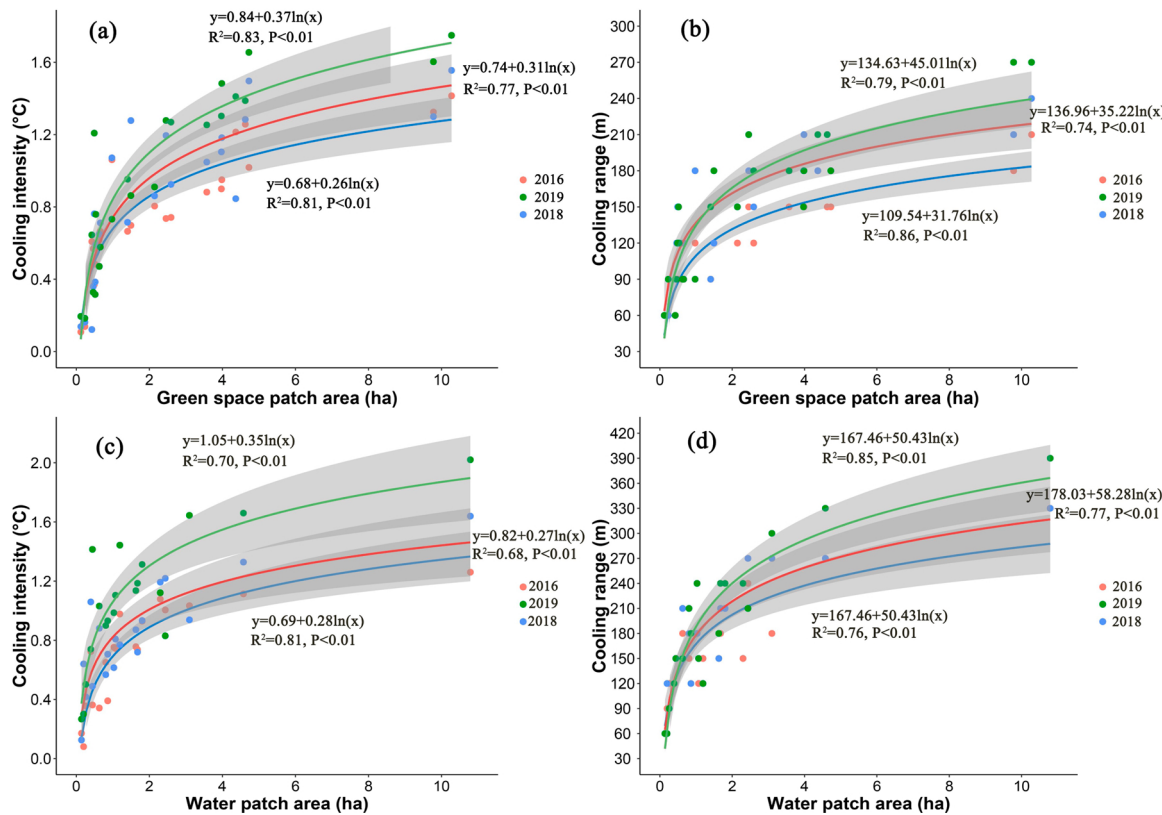


Fig. 7. (a-d) Relationship between (a) cooling intensity and tree-based green space patch area, (b) cooling range and tree-based green space patch area, (c) cooling intensity and water patch area, and (d) cooling range and water patch area from 2016 to 2019. (For interpretation of the references to colour in this figure legend, the reader is referred to the web version of this article).

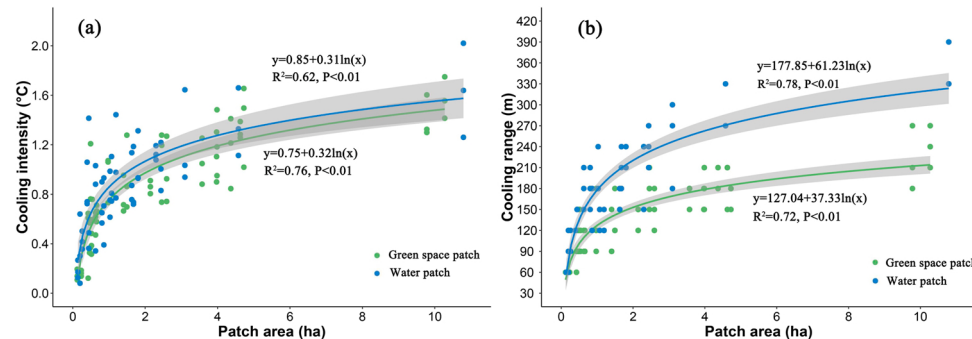


Fig. 8. (a-b) Comparison of the relationship between (a) cooling intensity and patch area of tree-based green space and water bodies and (b) cooling range and patch area of tree-based green space and water bodies. (For interpretation of the references to colour in this figure legend, the reader is referred to the web version of this article).

Table 3

Pearson correlation and partial correlation coefficients between mean LST and landscape metrics at the landscape level.

	PLAND	SHAPE_MN	FRAC_MN	AI
Pearson correlation	Green space	-0.600**	-0.643**	-0.644**
	Water body	-0.295**	-0.366**	-0.363**
Partial correlation	Green space	-0.303**	0.112*	0.082
	Water body	-0.177**	0.137**	-0.018
				0.207**

**Correlation is significant at the 0.01 level (2-tailed).

*Correlation is significant at the 0.05 level (2-tailed).

and land cover was more complex (Yan et al., 2018). To minimize the influence of these external factors, tree-based green spaces and water patches with homogenous and dense surrounding buildings were chosen here. Furthermore, according to the time data collected as determined by the Landsat images of our study area, the results derived in this study were in the daytime when the UHI and cooling effect were relatively significant.

4.3. Implications for urban green space and water design and planning

At the landscape level, the results from Section 3.3 show that the effect of green spaces and water bodies on the mean LST of urbanized areas was mainly influenced by their area, shape complexity, and aggregation. High proportions of green spaces and water bodies contribute

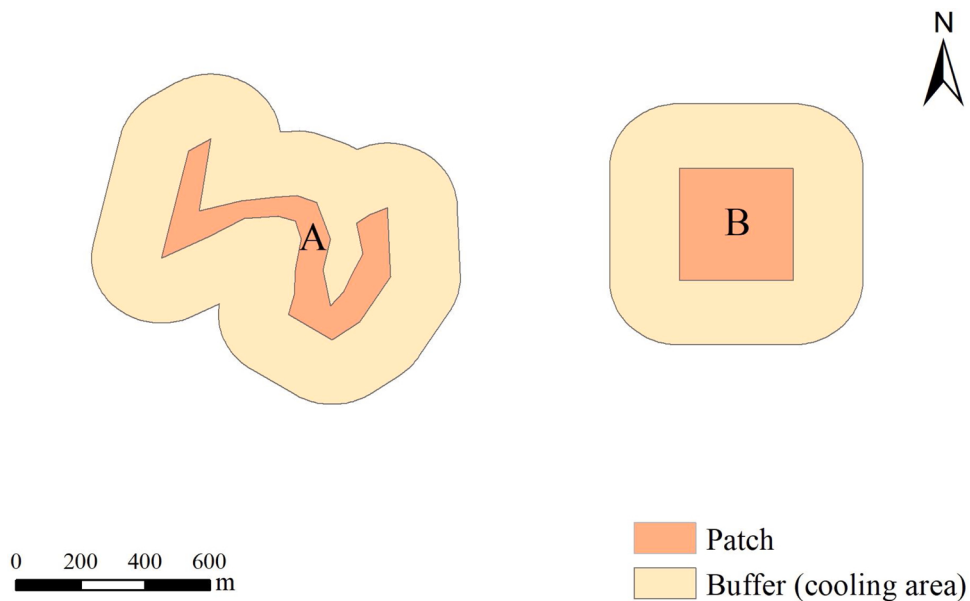


Fig. 9. Cooling areas of patches with the same area but different PSIs.

to a low LST. A 10 % increase in green space cover results in a 0.39°C decrease in the mean LST of urbanized areas, while a 0.42°C decrease occurs with the same increase in water cover. In addition, the aggregation of green spaces and water bodies is another important factor for their cooling effect. Compared to aggregated green spaces or water bodies, more fragmented green spaces or water bodies may be preferable for reducing the mean LST. Furthermore, the shape complexity of green spaces and water bodies is positively correlated with their surrounding LST, indicating that green and blue spaces with simpler shapes may cool the surrounding environment more than those with more complex shapes.

At the patch level, as two main characteristics of green space and water patches, the area and PSI have different effects on their cooling ranges and intensities. As we discussed in Section 4.2, the area of green spaces and water patches is the most important element for explaining the increasing cooling range and intensity. However, although the cooling effect is enhanced as patch size increases, there is a TVoE according to the "law of diminishing marginal utility" in economics (Yu et al., 2017). Within a certain range, increasing the patch area leads to a significant improvement in its cooling effect. Once its area exceeds the threshold value, the increase in the cooling effect is very small. Our results suggest that increasing the area of tree-based green space and water patches within approximately 0.32 ha and 0.31 ha can effectively enhance their cooling intensity. In addition, the changes in PSI of both tree-based green space and water patches do not seem to impact their cooling effect.

Although the shape complexity of cold islands was not identified as a factor associated with their cooling effect at both the landscape and patch levels, as we discussed in Section 4.2, green spaces or water bodies with the same area but more complex shapes are suggested due to the more extensive cooling area they cover, which is of great significance in urbanized areas generally lacking sufficient spaces to create all green spaces and water bodies they need. During urban blue-green space planning in Nanning and other cities in the same climate zone, first, according to cooling demand, an appropriate proportion of green space or water cover at the landscape level can be determined based on the cooling caused by the increase in green space or water cover per unit. Then, the economic and effective size of tree-based green space or water patches is identified based on the TVoE. Furthermore, to ensure that the whole urbanized area will benefit from cold islands, the spatial distribution of green space and water patches can be suggested by their

different cooling ranges and cooling intensities (Fig. 10).

4.4. Limitations and future work

Several limitations of this study should be mentioned. First, the LST and landscape metrics extracted from remote sensing data are less accurate than those extracted from field measured data. Moreover, due to the poor quality of Landsat satellite images in Nanning, China in June, July and August, the Landsat satellite image used in this study was from October, when the cooling effect of green spaces and water bodies is not as significant as that in summer when the UHI is the most severe. Second, to avoid the interactions of the cooling effect between green space patches and water patches, a limited number of patches was selected based on the principles in Section 2.3. Therefore, more samples from other regions within the same climate zone are needed to conclude more interesting findings. Despite these limitations, the methodology adopted in this study is suggested to be robust, and most of the results drawn from this study are consistent with other published research, which can be reliable references for planning decision-making.

5. Conclusions

By investigating green spaces and water bodies in the urbanized areas of a subtropical city, Nanning, China, this study compared their cooling effect in terms of cooling range and cooling intensity, examined the difference in landscape-metric impacts on the cooling effect of green spaces and water bodies, and identified the economically optimal tree-based green space and water patch sizes for enhancing their cooling effect. Furthermore, based on the results, we proposed methods for planning urban blue-green spaces, which suggested that whether for green spaces or water bodies, the area-related metrics have a positive influence on their cooling effect. Furthermore, a 10 % increase in green space cover leads to a 0.39°C mean LST drop, while an additional 10 % water cover leads to a 0.42°C decrease in the mean LST. In addition, green spaces and water bodies with more complex shapes should be planned due to the more extensive cooling areas they create. Meanwhile, more fragmented green spaces and water bodies are preferable for reducing the LST. For green space patch and water patch planning, the economically optimal tree-based green space and water patch sizes are 0.32 ha and 0.31 ha, respectively, in Nanning. With the same area, a water patch is more likely to be established due to its slightly higher

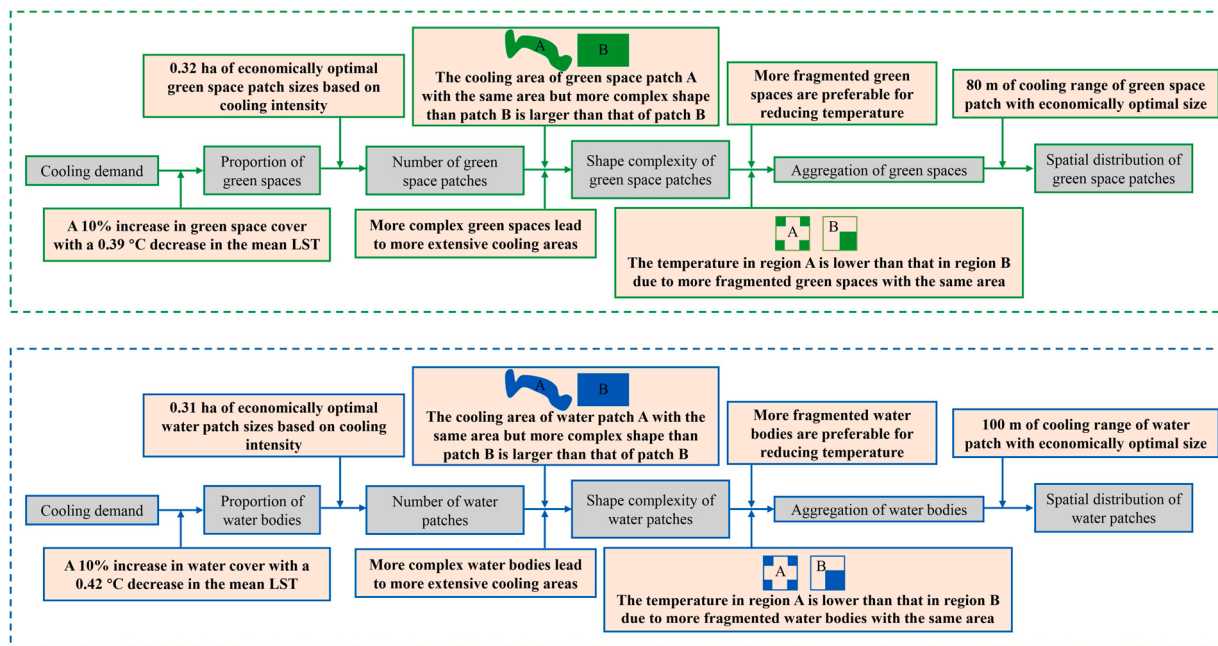


Fig. 10. Flow chart of urban blue-green space planning applicable to Nanning, the subtropical city proposed in this study.

cooling intensity and much larger cooling range than those of the tree-based green space patches. One contribution of this study is to systematically compare the cooling effect of urban green spaces and water bodies and the dominating influencing factors in the subtropical climate zone. The other contribution is to provide a clear practical technical framework for urban blue and green space planning from theoretical study for mitigating the UHI effect.

Declaration of Competing Interest

The authors declare that they have no known competing financial interests or personal relationships that could have appeared to influence the work reported in this paper.

Acknowledgements

This work was supported by research grants from National Natural Science Foundation of China (71964002), Natural Science Foundation of Guangxi Province (2018GXNSFAA050040), Humanities and Social Science Fund of Ministry of Education of China (17YJCZH153), and Scientific Research Foundation of Guangxi University (XGZ150300).

Appendix A. Supplementary data

Supplementary material related to this article can be found, in the online version, at doi:<https://doi.org/10.1016/j.scs.2021.102711>.

References

- Akbari, H., & Kolokotsa, D. (2016). Three decades of urban heat islands and mitigation technologies research. *Energy and Buildings*, *133*, 834–842.
- Amani-Beni, M., Zhang, B., Xie, G.-d., & Xu, J. (2018). Impact of urban park's tree, grass and waterbody on microclimate in hot summer days: a case study of Olympic Park in Beijing, China. *Urban Forestry & Urban Greening*, *32*, 1–6.
- Artis, D. A., & Carnahan, W. H. (1982). Survey of emissivity variability in thermography of urban areas. *Remote Sensing of Environment*, *12*, 313–329.
- Asgarian, A., Amiri, B. J., & Sakieh, Y. (2015). Assessing the effect of green cover spatial patterns on urban land surface temperature using landscape metrics approach. *Urban Ecosystems*, *18*, 209–222.
- Bao, T., Li, X., Zhang, J., Zhang, Y., & Tian, S. (2016). Assessing the distribution of urban green spaces and its anisotropic cooling distance on urban heat island pattern in Baotou, China. *ISPRS International Journal of Geo-information*, *5*, 12.
- Brown, R. D., Vanos, J., Kenny, N., & Lenzholzer, S. (2015). Designing urban parks that ameliorate the effects of climate change. *Landscape and Urban Planning*, *138*, 118–131.
- Buyantuyev, A., & Wu, J. (2010). Urban heat islands and landscape heterogeneity: Linking spatiotemporal variations in surface temperatures to land-cover and socioeconomic patterns. *Landscape Ecology*, *25*, 17–33.
- Ca, V. T., Asaeda, T., & Abu, E. M. (1998). Reductions in air conditioning energy caused by a nearby park. *Energy and Buildings*, *29*, 83–92.
- Cai, Z., Han, G., & Chen, M. (2018). Do water bodies play an important role in the relationship between urban form and land surface temperature? *Sustainable Cities and Society*, *39*, 487–498.
- Cao, Q., Yu, D., Georgescu, M., Wu, J., & Wang, W. (2018). Impacts of future urban expansion on summer climate and heat-related human health in eastern China. *Environment International*, *112*, 134–146.
- Chander, G., Helder, D. L., Markham, B. L., Dewald, J. D., Kaita, E., Thome, K. J., et al. (2004). Landsat-5 TM reflective-band absolute radiometric calibration. *IEEE Transactions on Geoscience and Remote Sensing*, *42*, 2747–2760.
- Chang, C. R., Li, M. H., & Chang, S. D. (2007). A preliminary study on the local cool-island intensity of Taipei city parks. *Landscape and Urban Planning*, *80*, 386–395.
- Chen, A., Yao, X. A., Sun, R., & Chen, L. (2014). Effect of urban green patterns on surface urban cool islands and its seasonal variations. *Urban Forestry & Urban Greening*, *13*, 646–654.
- Chen, X. L., Zhao, H. M., Li, P. X., & Yin, Z. Y. (2006). Remote sensing image-based analysis of the relationship between urban heat island and land use/cover changes. *Remote Sensing of Environment*, *104*, 133–146.
- Doick, K. J., Peace, A., & Hutchings, T. R. (2014). The role of one large greenspace in mitigating London's nocturnal urban heat island. *The Science of the Total Environment*, *493*, 662–671.
- Du, H., Cai, W., Xu, Y., Wang, Z., Wang, Y., & Cai, Y. (2017). Quantifying the cool island effects of urban green spaces using remote sensing data. *Urban Forestry & Urban Greening*, *27*, 24–31.
- Du, H., Song, X., Jiang, H., Kan, Z., Wang, Z., & Cai, Y. (2016). Research on the cooling island effects of water body: A case study of Shanghai China. *Ecological Indicators*, *67*, 31–38.
- Estoque, R. C., Murayama, Y., & Myint, S. W. (2017). Effects of landscape composition and pattern on land surface temperature: An urban heat island study in the megacities of Southeast Asia. *The Science of the Total Environment*, *577*, 349–359.
- Fan, H., Yu, Z., Yang, G., Liu, T. Y., Liu, T. Y., Hung, C. H., et al. (2019). How to cool hot-humid (Asian) cities with urban trees? An optimal landscape size perspective. *Agricultural and Forest Meteorology*, *265*, 338–348.
- Feng, X. G., & Shi, H. (2012). Research on the cooling effect of Xi'an parks in summer based on remote sensing. *Acta Ecologica Sinica*, *32*, 7355–7363.
- Gunawardena, K. R., Wells, M. J., & Kershaw, T. (2017). Utilising green and bluespace to mitigate urban heat island intensity. *The Science of the Total Environment*, *1040*, 584–585.
- Hamada, S., & Ohta, T. (2010). Seasonal variations in the cooling effect of urban green areas on surrounding urban areas. *Urban Forestry & Urban Greening*, *9*, 15–24.
- Hathaway, E. A., & Sharples, S. (2012). The interaction of rivers and urban form in mitigating the urban heat island effect: A UK case study. *Building and Environment*, *58*, 14–22.
- Huang, M., Cui, P., & He, X. (2018). Study of the cooling effects of urban green space in Harbin in terms of reducing the heat island effect. *Sustainability*, *10*, 1101.

- Jaganmohan, M., Knapp, S., Buchmann, C. M., & Schwarz, N. (2016). The bigger, the better? The influence of urban green space design on cooling effects for residential areas. *Journal of Environmental Quality*, 45, 134–145.
- Jauregui, E. (1991). Influence of a large urban park on temperature and convective precipitation in a tropical city. *Energy and Buildings*, 15, 457–463.
- Kong, F., Yin, H., James, P., Hutyra, L. R., & He, H. S. (2014). Effects of spatial pattern of greenspace on urban cooling in a large metropolitan area of eastern China. *Landscape and Urban Planning*, 128, 35–47.
- Lau, S. S., Lin, P., & Qin, H. (2012). A preliminary study on environmental performances of pocket parks in high-rise and high-density urban context in Hong Kong. *International Journal of Low-Carbon Technologies*, 7, 215–225.
- Lee, S. H., Lee, K. S., Jin, W. C., & Song, H. K. (2009). Effect of an urban park on air temperature differences in a central business district area. *Landscape and Ecological Engineering*, 5, 183–191.
- Li, J., Song, C., Cao, L., Zhu, F., Meng, X., & Wu, J. (2011). Impacts of landscape structure on surface urban heat islands: a case study of Shanghai, China. *Remote Sensing of Environment*, 115, 3249–3263.
- Li, X., Zhou, W., Ouyang, Z., Xu, W., & Zheng, H. (2012). Spatial pattern of greenspace affects land surface temperature: evidence from the heavily urbanized Beijing metropolitan area, China. *Landscape Ecology*, 27, 887–898.
- Lin, W., Yu, T., Chang, X., Wu, W., & Zhang, Y. (2015). Calculating cooling extents of green parks using remote sensing: Method and test. *Landscape and Urban Planning*, 134, 66–75.
- Maimaitiyiming, M., Ghulam, A., Tiyip, T., Pla, F., Latorre-Carmona, P., Halik, Ü., et al. (2014). Effects of green space spatial pattern on land surface temperature: Implications for sustainable urban planning and climate change adaptation. *ISPRS Journal of Photogrammetry and Remote Sensing*, 89, 59–66.
- Masoudi, M., & Tan, P. Y. (2019). Multi-year comparison of the effects of spatial pattern of urban green spaces on urban land surface temperature. *Landscape and Urban Planning*, 184, 44–58.
- Masoudi, M., Tan, P. Y., & Liew, S. C. (2019). Multi-city comparison of the relationships between spatial pattern and cooling effect of urban green spaces in four major Asian cities. *Ecological Indicators*, 98, 200–213.
- Monteiro, M. V., Doick, K. J., Handley, P., & Peace, A. (2016). The impact of greenspace size on the extent of local nocturnal air temperature cooling in London. *Urban Forestry & Urban Greening*, 16, 160–169.
- Moss, J. L., Doick, K. J., Smith, S., & Shahrestani, M. (2019). Influence of evaporative cooling by urban forests on cooling demand in cities. *Urban Forestry & Urban Greening*, 37, 65–73.
- Murakawa, S., Sekine, T., Narita, K. I., & Nishina, D. (1991). Study of the effects of a river on the thermal environment in an urban area. *Energy and Buildings*, 16, 993–1001.
- Nanning Municipal Administration Bureau. (2019). <http://nnyj.nanning.gov.cn/>, accessed 5.29.2019.
- Nanning Municipal Statistics Bureau. (2018). *Nanjing Statistical Yearbook*. Beijing, China: China Statistics Press (in Chinese).
- NASA (1998-01-06/2005-09-20). Science date users handbook[EB/OL] http://ltpwww.gsfc.nasa.gov/IAS/handbook/handbook_toc.html.
- Oliveira, S., Andrade, H., & Vaz, T. (2011). The cooling effect of green spaces as a contribution to the mitigation of urban heat: A case study in Lisbon. *Building and Environment*, 46, 2186–2194.
- Qin, Z., Li, W., Gao, M., & Zhang, H. (2006). Estimation of land surface emissivity for landsat TM6 and its application to lingxian region in north China. In *Remote sensing for environmental monitoring, GIS applications, and geology VI* (vol. 6366). International Society for Optics and Photonics, Article 636618.
- Sun, Y., & Augenbroe, G. (2014). Urban heat island effect on energy application studies of office buildings. *Energy Building*, 77, 171–179.
- Sun, R., & Chen, L. (2012). How can urban water bodies be designed for climate adaptation? *Landscape and Urban Planning*, 105, 27–33.
- Sun, R., Chen, A., Chen, L., & Lü, Y. (2012). Cooling effects of wetlands in an urban region: The case of Beijing. *Ecological Indicators*, 20, 57–64.
- Sun, R., Chen, L., & Braat, L. C. (2017). Effects of green space dynamics on urban heat islands: Mitigation and diversification. *Ecosystem Services*, 23, 38–46.
- Syafii, N. I., Ichinose, M., Kumakura, E., Jusuf, S. K., Chigusa, K., & Wong, N. H. (2017). Thermal environment assessment around bodies of water in urban canyons: A scale model study. *Sustainable Cities and Society*, 34, 79–89.
- Topalar, Y., Blocken, B., Maiheu, B., & Heijst van, G. J. F. (2018). The effect of an urban park on the microclimate in its vicinity: A case study for Antwerp, Belgium. *International Journal of Climatology*, 38, e303–e322.
- Wu, D., Wang, Y., Fan, C., & Xia, B. (2018). Thermal environment effects and interactions of reservoirs and forests as urban blue-green infrastructures. *Ecological Indicators*, 91, 657–663.
- Xie, M., Wang, Y., Chang, Q., Fu, M., & Ye, M. (2013). Assessment of landscape patterns affecting land surface temperature in different biophysical gradients in Shenzhen, China. *Urban Ecosystems*, 16, 871–886.
- Xue, Z., Hou, G., Zhang, Z., Lyu, X., Jiang, M., Zou, Y., et al. (2019). Quantifying the cooling-effects of urban and peri-urban wetlands using remote sensing data: Case study of cities of Northeast China. *Landscape and Urban Planning*, 182, 92–100.
- Yan, H., Wu, F., & Dong, L. (2018). Influence of a large urban park on the local urban thermal environment. *The Science of the Total Environment*, 622, 882–891.
- Yang, G., Yu, Z., Jørgensen, G., & Vejre, H. (2020). How can urban blue-green space be planned for climate adaption in high-latitude cities? A seasonal perspective. *Sustainable Cities and Society*, 53, Article 101932.
- Yu, Z., Guo, Q., & Sun, R. (2015). Impact of urban cooling effect based on landscape scale: A review. *Chinese Journal of Applied Ecology*, 26, 636–642.
- Yu, Z., Guo, X., Jørgensen, G., & Vejre, H. (2017). How can urban green spaces be planned for climate adaptation in subtropical cities? *Ecological Indicators*, 82, 152–162.
- Yu, Z., Guo, X., Zeng, Y., Koga, M., & Vejre, H. (2018). Variations in land surface temperature and cooling efficiency of green space in rapid urbanization: The case of Fuzhou city, China. *Urban Forestry & Urban Greening*, 29, 113–121.
- Zhang, Y., Murray, A. T., & Turner, B. L. (2017). Optimizing green space locations to reduce daytime and nighttime urban heat island effects in Phoenix, Arizona. *Landscape and Urban Planning*, 165, 162–171.
- Zhang, Y., Odeh, I. O. A., & Ramadan, E. (2013). Assessment of land surface temperature in relation to landscape metrics and fractional vegetation cover in an urban/peri-urban region using Landsat data. *International Journal of Remote Sensing*, 34, 168–189.
- Zhou, X., & Wang, Y. C. (2011). Dynamics of land surface temperature in response to landuse/cover change. *Geographical Research*, 49, 23–36.
- Zhou, W., Cao, F., & Wang, G. (2019). Effects of spatial pattern of forest vegetation on urban cooling in a compact megacity. *Forests*, 10, 282.
- Zhou, W., Qian, Y., Li, X., Li, W., & Han, L. (2014). Relationships between land cover and the surface urban heat island: Seasonal variability and effects of spatial and thematic resolution of land cover data on predicting land surface temperatures. *Landscape Ecology*, 29, 153–167.